

# A GENERATIVE MODELING / PHYSICS-INFORMED NEURAL NETWORK APPROACH TO RANDOM DIFFERENTIAL EQUATIONS

Georgios Arampatzis<sup>1,2</sup>, Stylianos Katsarakis<sup>2</sup> and Charalambos Makridakis<sup>2,3</sup>

<sup>1</sup> DMAM, University of Crete, Greece

<sup>2</sup> IACM-FORTH, Greece

<sup>3</sup> MPS, University of Sussex, United Kingdom

## Abstract

The integration of Scientific Machine Learning (SciML) techniques with uncertainty quantification (UQ) represents a rapidly evolving frontier in computational science. This work advances Physics-Informed Neural Networks (PINNs) by incorporating probabilistic frameworks to effectively model uncertainty in complex systems. Our approach enhances the representation of uncertainty in forward problems by combining generative modeling techniques with PINNs. This integration enables in a systematic fashion uncertainty control while maintaining the predictive accuracy of the model. We demonstrate the utility of this method through applications to random differential equations and random partial differential equations (PDEs).

## 1 Introduction

### 1.1 Problem Formulation and Approach

In this paper, we consider random differential equations, which are differential equations that depend on random parameters. Assuming that we have knowledge of the probability distribution of these parameters, we aim to assess the probability distribution of the solutions. This is a fundamental problem in uncertainty quantification and can be regarded as the initial step in designing algorithms for more intricate inverse problems where we aim to determine both the form of the equation and its solutions with controlled uncertainty by leveraging the available data.

The primary tools we will employ include discrete neural network methods and generative models, along with adaptations of ideas from Physics-Informed Neural Networks tailored to our current problem. Machine learning and neural networks have proven to be highly effective tools for approximating probability distributions in  $\mathbb{R}^k$ , even for large dimensions  $k$ . However, the solutions of random differential equations can be viewed as probability distributions on infinite-dimensional spaces (typically Hilbert or Sobolev spaces), making their formulation and approximation particularly intricate. This is one of the key issues we aim to address in the present work.

The problems we consider have the form

$$\mathcal{A}_\xi u(\cdot, \xi) = \mathcal{F}_\xi, \quad (1)$$

where  $\mathcal{A}_\xi$  is a  $\xi$ -parametrised differential operator (incorporating possible initial and boundary conditions), and  $\mathcal{F}_\xi$  is the source. For each fixed  $\xi$ ,  $u(\cdot; \xi)$  denotes the solution of the differential equation, which we interpret as a mapping  $U : \Xi \rightarrow \mathcal{H}$  with  $U(\xi) := u(\cdot, \xi)$ . The space  $\mathcal{H}$  where  $u$  takes values for each  $\xi$  is an (infinite dimensional) Hilbert or Sobolev space. We assume that the

random parameter  $\xi \in \Xi$  is distributed according to a known Borel probability measure  $\gamma$  on  $\Xi$ . Our aim is to approximate the random variable  $U$  and its law  $\nu_u \in \mathcal{P}(\mathcal{H})$ ; here  $\mathcal{P}(\mathcal{X})$  denotes the set of Borel probability measures on  $\mathcal{X}$ .

### Motivation and Neural Measures

One of the key successes of neural network methods is their ability to effectively approximate probability distributions. In fact, several important problems of interest rely on generating a probability distribution when the available data represent specific instances of the unknown distribution. Typically, if the data is represented by an empirical measure  $\nu_{\text{Dat}} \in \mathcal{P}(\mathbb{R}^k)$ , we would like to generate an approximation of  $\nu_{\text{True}} \in \mathcal{P}(\mathbb{R}^k)$  by optimising

$$\min_{\mu \in V_{\Theta}} d_{\mathcal{M}}(\mu, \nu_{\text{Dat}}), \quad (2)$$

where  $V_{\Theta}$  are appropriate discrete subsets of  $\mathcal{P}(\mathbb{R}^k)$  determined by a parameter set  $\Theta$  which is connected in an appropriate manner with neural network sets of given architecture and  $d_{\mathcal{M}}(\cdot, \cdot)$  a specified distance (or divergence) on  $\mathcal{P}(\mathbb{R}^k)$ . We then hope that

$$\mu_{\theta^*} \cong \nu_{\text{True}}, \quad \text{where } \mu_{\theta^*} \in \arg \min_{\mu \in V_{\Theta}} d_{\mathcal{M}}(\mu, \nu_{\text{Dat}}). \quad (3)$$

Representative works utilising the aforementioned generative model framework for a variety of applications include [1, 4, 8, 13, 15, 48], and the references in [45]. For a recent modelling perspective that interprets various generative models as mean field games, see [45].

The above framework relies on various alternative choices, each one yielding fundamentally distinct algorithms at the end. We would like to explore the potential extension of this approach to approximate solutions of (1). To accomplish this we must first systematically construct discrete spaces  $V_{\Theta}$  such that  $V_{\Theta} \subset \mathcal{P}(\mathcal{H})$ . We adopt the following alternative approaches:

- fully NN based  $V_{\Theta}$ , detailed in Section 3.1
- Polynomial Chaos Expansion (PCE)-NN  $V_{\Theta}$ , detailed in Section 3.2
- Galerkin-NN  $V_{\Theta}$ , detailed in Section 3.3 .

### Incorporating PINNs

Once appropriate  $V_{\Theta}$ ,  $V_{\Theta} \subset \mathcal{P}(\mathcal{H})$ , are in place, one may want to incorporate the key idea of Physics Informed Neural Networks and to combine it with the Neural Measure spaces. In fact, one needs to define

$$\mathcal{A} \odot \mu, \quad \mu \in V_{\Theta} \subset \mathcal{P}(\mathcal{H}), \quad (4)$$

i.e. the probability distribution on  $\mathcal{P}(\mathcal{H}^{\text{imag}})$ , which is obtained by applying  $\mathcal{A}_{\xi}$  to  $\mu$  in an appropriate sense. Here  $\mathcal{A}_{\xi}u(\cdot, \xi)$ ,  $\mathcal{F}_{\xi} \in \mathcal{H}^{\text{imag}}$  for each fixed  $\xi$ . This definition is made precise in Sections 2.3 and 2.4.

We then consider the abstract problem,

$$\min_{\mu \in V_{\Theta}} d_{\tilde{\mathcal{M}}}(\mathcal{A} \odot \mu, \nu_{\mathcal{F}}), \quad (5)$$

where  $\nu_{\mathcal{F}} \in \mathcal{P}(\mathcal{H}^{\text{imag}})$  is the distribution corresponding to the source  $\mathcal{F}_{\xi}$ , and  $d_{\tilde{\mathcal{M}}}(\cdot, \cdot)$  a specified distance (or divergence) on  $\mathcal{P}(\mathcal{H}^{\text{imag}})$ .

## Formulation of the methods and results

The plan outlined above is implemented systematically in the following sections. We adopt a concrete yet somewhat abstract approach for two main reasons:

(a) *the formulation of discrete neural measure spaces has the potential to be valuable in various other applications of uncertainty quantification (UQ) for partial differential equations (PDEs), and*

(b) *the integration of the physics-informed neural networks (PINN) framework into the final algorithms can be carried out in a general manner, independent of the specific choice of measure metrics.*

We then show that employing Wasserstein distances offers particular advantages in the implementation of the final algorithms.

This work is structured to systematically develop and analyse a generative modelling approach for Uncertainty Quantification using Physics-Informed Neural Networks (PINNs). In Section 2, we introduce the underlying problem, and the corresponding probabilistic framework essential to our study. Next, we introduce new notational conventions and the variational formulation used. The variational principle forms the backbone of our approach, guiding the optimisation process for learning the solution distribution of the random differential equation. Section 3 presents the model construction in detail. We define a fundamental representation of Neural Measures tailored to the problem’s probabilistic nature and explore three distinct architectural frameworks, namely fully discrete randomised neural networks, Polynomial Chaos Expansion Neural Networks (PCE-NN), Galerkin-based neural networks. In Section 4, we shift focus to the variational distances used during training, with particular emphasis on the Wasserstein distance and its interpretation in terms of Dirac measures, which naturally relate it to  $L^p$ -type loss functionals. We also discuss alternative metrics and divergences that can be integrated into the framework. Section 5 presents numerical experiments that validate the proposed framework across three representative problems: a bistable ODE, a linear diffusion PDE, and a reaction-diffusion PDE. In each case, the problem parameters are treated as random variables, and the aim is to learn the distribution of the solution. The results demonstrate that the generative PINN models can accurately capture both the mean and higher-order statistical properties of the solutions. Comparisons with reference solvers show very good qualitative and quantitative agreement, though challenges arise in representing sharply peaked distributions and boundary behaviours. Different architectures, including standard PINNs and PINN-PCE variants, are assessed in terms of convergence, error behaviour, and their effectiveness in representing uncertainty. Finally, Section 6 provides formal definitions and foundational elements used throughout the work.

## Previous works

Physics-Informed Neural Networks (PINNs) are a class of neural network-based methods designed to approximate solutions of partial differential equations (PDEs), where the loss function incorporates the residual of the PDE [33]. Similar approaches have been explored in [5, 20, 26, 34, 38],

To the best of our knowledge, the systematic framework presented here is novel. However, a number of related studies share certain aspects with our approach. A review of neural network approaches to uncertainty quantification can be found in [32]. A method which uses the PINN framework for random differential equations is presented as well. It is assumed the approximate solution is distributed with a normal distribution and the method provides ways to estimate its mean and variance. Inferencing stochastic solution and parameters of a Random PDE, by combining Polynomial Chaos Expansions, [42], and PCA we considered in [46, 47], other related works include [30]. Physics Informed Generative Adversarial Networks were considered in [12] and [44].

See also [17, 27, 40], for UQ related approaches. Neural Operators to address certain issues involving stochasticity in approximating PDEs in infinite dimensional setting include [14, 18, 19, 21, 23, 25, 35], approaches were proposed in [10, 22, 24, 43], their new role and importance in application to sciences was discussed in [11].

## 2 The problem and its probabilistic framework

### 2.1 Problem and Assumptions

The objective is to approximate the probability distribution associated with the solution of the following Random (PDE):

$$\begin{aligned} A_\xi u(x, t; \xi) &= f(x, t; \xi) \quad \forall (x, t) \in D \times (0, T] \\ B_\xi u(x, t; \xi) &= g(x, t; \xi) \quad \forall (x, t) \in \Gamma \end{aligned} \quad (6)$$

where  $u(x, t; \xi)$  denotes the solution of the PDE, which we interpret as the mapping  $U : \Xi \rightarrow \mathcal{H}$  with  $U(\xi) := u(\cdot, \cdot; \xi)$ . Here,  $A_\xi : \mathcal{H} \rightarrow \tilde{\mathcal{H}}$  is a  $\xi$ -parametrised differential operator, and  $B_\xi : \mathcal{H} \rightarrow \bar{\mathcal{H}}$  is the associated boundary operator. The random parameter  $\xi \in \Xi$  is distributed according to a Borel probability measure  $\gamma$  on  $\Xi$ .

Analysing the behaviour of solutions is beyond the scope of this work. Our objective is to propose numerical algorithms for approximating the distribution associated with the solution of the problems at hand. Therefore, we assume that the solution to (6) exists and is sufficiently regular for our purposes. In particular, we assume throughout that

- The operators  $A_\xi$  and  $B_\xi$  are well-defined for  $\gamma$ -almost every  $\xi$ , and the solution of (6) belongs in  $L^2(\gamma; \mathcal{H})$ .
- For  $q \in L^2(\gamma; \mathcal{H})$ , we assume that the following maps:

$$\begin{aligned} A\mathcal{Q}(\xi) &:= A_\xi q(\xi), \quad B\mathcal{Q}(\xi) := B_\xi q(\xi) \quad \text{are } L^2\text{-integrable, i.e.,} \\ A\mathcal{Q} &\in L^2(\gamma; \tilde{\mathcal{H}}) \quad \text{and} \quad B\mathcal{Q} \in L^2(\gamma; \bar{\mathcal{H}}). \end{aligned} \quad (7)$$

Where the space  $L^2(\gamma; \mathcal{H})$  is defined in the sense of Bochner integration, see for example Section 7.2.2 of [9] for details. In particular this implies that

$$\int \|U(\xi)\|_{\mathcal{H}}^2 \gamma(d\xi) < \infty.$$

and we denote by  $U$  the element of  $L^2(\gamma; \mathcal{H})$ , corresponding to the solution  $u$ . Using the definition of pushforward, we define its probability measure  $\nu_u \in \mathcal{P}(\mathcal{H})$  by

$$\nu_u(A) = [U]_{\#} \gamma(A) = \gamma \circ U^{-1}(A), \quad \forall A \in \mathcal{B}(\mathcal{H}).$$

Since we assume  $U \in L^2(\gamma; \mathcal{H})$ , this probability has a finite second moment.

In the next Sections, we introduce a variational method based on a parametrised family of Neural Models to construct an approximation of the target probability distribution  $\nu_u$ .

### 2.2 Probabilistic framework

We review some standard concepts from probability theory which will be useful in the sequel. We begin by assuming an abstract probability space  $(\Omega, \mathcal{F}, \mathbb{P})$ , a measurable space over  $\mathcal{H}$ , eg.

$(\mathcal{H}, \mathcal{B}(\mathcal{H}))$ , and a random element  $\tilde{q} : \Omega \rightarrow \mathcal{H}$ , ie.  $\mathcal{F}/\mathcal{B}(\mathcal{H})$ –measurable function. The law of  $\tilde{q}$  is the pushforward measure of  $\mathbb{P}$  under  $\tilde{q}$ , defined as:

$$[\tilde{q}]_{\#} \mathbb{P}(A) = \mathbb{P}(\tilde{q} \in A) = \mathbb{P} \circ \tilde{q}^{-1}(A), \quad A \in \mathcal{B}(\mathcal{H}),$$

where  $\tilde{q}^{-1}$  denotes the preimage of the set  $A$ . It is straightforward to verify that this defines a valid probability measure.

An important assumption in our setting is that we only consider solutions such that  $u \in L^2(\gamma; \mathcal{H})$ , which ensures two key properties:

- The mapping  $U(\xi) = u(\cdot; \xi)$  is measurable with respect to  $\xi$ ,
- $U(\xi)$  has a finite second moment with respect to  $\gamma$ .

Let  $\xi : \Omega \rightarrow \Xi$  be a random element ( ie.  $\mathcal{F}/\mathcal{B}(\Xi)$ –measurable function) with law  $\gamma$ . We are interested in random elements  $\tilde{q}$  expressible as compositions of a function  $q \in L^2(\gamma; \mathcal{H})$  and  $\xi$ , ie.

$$\tilde{q}(\omega) = q(\xi(\omega)), \quad \mathbb{P} - \text{as } \omega. \quad (8)$$

It is also straightforward to verify that  $\tilde{q}$  has a finite second moment with respect to  $\mathbb{P}$ , and its law satisfies:

$$[\tilde{q}]_{\#} \mathbb{P}(A) = [q]_{\#} \gamma(A), \quad \forall A \in \mathcal{B}(\mathcal{H}).$$

Hence setting  $\nu_q := [q]_{\#} \gamma$  we have

$$\nu_q = [q]_{\#} \gamma \in \mathcal{P}(\mathcal{H}),$$

where  $\mathcal{P}(\mathcal{H})$  denotes the set of all Borel probability measures on  $\mathcal{H}$ , ie. measures defined on  $(\mathcal{H}, \mathcal{B}(\mathcal{H}))$ .

Since our goal is to approximate probability measures, we introduce the following collections:

- For  $p \geq 1$ , define the sub-collection  $\mathcal{P}_p(\mathcal{H})$  consisting of all measures with finite  $p$ –th moment,

$$\mathcal{P}_p(\mathcal{H}) := \left\{ \mu \in \mathcal{P}(\mathcal{H}) : \int_{\mathcal{H}} d_{\mathcal{H}}(h, \bar{h})^p \mu(dh) < \infty \quad \text{for some (and hence any) } \bar{h} \in \tilde{\mathcal{H}} \right\}$$

where  $(\mathcal{H}, d_{\mathcal{H}})$  is the metric space generating the Borel  $\sigma$ –algebra  $\mathcal{B}(\mathcal{H})$ .

- Given a reference measure  $\gamma$  on  $\mathcal{B}(\Xi)$ , define sub-collection of  $\mathcal{P}_2(\mathcal{H})$

$$\mathcal{P}_p^{\gamma}(\mathcal{H}) = \left\{ \mu \in \mathcal{P}(\mathcal{H}) : \mu = [X]_{\#} \gamma \text{ for some } X \in L^p(\gamma; \mathcal{H}) \right\}.$$

Over those collections, one may consider alternative metrics for distances or divergences. In this work, we shall use the Wasserstein distance  $W_p$ , [2, 41] and the corresponding  $(\mathcal{P}_p(\mathcal{H}), W_p)$  metric space. The  $p$ –Wasserstein distance is given by

$$W_p(\mu, \nu) := \inf_{\pi \in \Pi(\mu, \nu)} \left( \int_{\mathcal{H} \times \mathcal{H}} d_{\mathcal{H}}(x, y)^p \pi(dx, dy) \right)^{1/p}, \quad (9)$$

where  $\Pi(\mu, \nu)$  is the set of all plans (joint distributions) with marginals  $\mu$  and  $\nu$ , [2]. Furthermore, we shall use the notation,

$$d_{p, \gamma}([X]_{\#} \gamma, [Y]_{\#} \gamma)^p := \int_{\mathcal{H} \times \mathcal{H}} d_{\mathcal{H}}(x, y)^p [(X, Y)]_{\#} \gamma(dx, dy) = \int_{\Xi} \|X(\xi) - Y(\xi)\|_{\mathcal{H}}^p \gamma(d\xi). \quad (10)$$

The distance  $d_{p, \gamma}$  induces a metric on  $L^p(\gamma; \mathcal{H})$ .

## 2.3 Transformed Law due to Parameterised Operators

We now introduce a notation to represent the law of expressions such as  $A_\xi q(\xi)$  and  $B_\xi q(\xi)$ . In the most general setting, one might define stochastic processes  $\tilde{A} : \Xi \times \mathcal{H} \rightarrow \tilde{\mathcal{H}}$  and  $\tilde{B} : \Xi \times \mathcal{H} \rightarrow \tilde{\mathcal{H}}$ , with appropriate measurability conditions. However, in Section 2.1, we simplify the setting by assuming hypothesis stated in (7), ensuring measurability. We then define the operation  $\odot$  as follows:

$$A \odot ([q]_{\#} \gamma)(C) := [A_\xi q(\xi)]_{\#} \mathbb{P}(C),$$

and similarly for the parameterised operator  $B_\xi$ . For instance we may rewrite the random PDE as equality of probability measures as follows,

$$A \odot \nu_u(C) = \nu_f(C) = [f(\cdot; \xi)]_{\#} \mathbb{P}(C), \quad \forall C \in \mathcal{B}(\tilde{\mathcal{H}}).$$

It will be useful to summarise these definitions as follows. We define and study metric spaces of Borel probability measures, such as  $\mathcal{P}_2^\gamma(\mathcal{H})$ ,  $\mathcal{P}_2^\gamma(\tilde{\mathcal{H}})$  and  $\mathcal{P}_2^\gamma(\overline{\mathcal{H}})$ , and decompose the law of the solution  $u$  into a measurable function  $U(\xi)$  and a probability measure  $\gamma$ , according to the diagram:

$$\mathbb{P} \xrightarrow{\xi} \gamma \begin{cases} \xrightarrow{q} [q]_{\#} \gamma \\ \xrightarrow{A \odot} A \odot [q]_{\#} \gamma \\ \xrightarrow{B \odot} B \odot [q]_{\#} \gamma \end{cases}$$

with

$$\begin{aligned} \mathbb{P} &\in \mathcal{P}(\Omega), \quad \gamma \in \mathcal{P}(\Xi), \quad [q]_{\#} \gamma \in \mathcal{P}_2^\gamma(\mathcal{H}) \\ A \odot [q]_{\#} \gamma &\in \mathcal{P}_2^\gamma(\tilde{\mathcal{H}}) \quad \text{and} \quad A \odot [q]_{\#} \gamma \in \mathcal{P}_2^\gamma(\overline{\mathcal{H}}). \end{aligned}$$

## 2.4 Variational Approximation of the Target Law

To approximate the target probability measure  $\nu_u$ , we adopt a variational approach. Specifically, we minimise a discrepancy functional over  $\mathcal{V}_\Theta = \mathcal{V}_\mathcal{N}^*$  that quantifies the difference between transformed distributions of the model and the target, induced by the operators  $A_\xi$  and  $B_\xi$ . Alternative specific choices for the neural measure spaces  $\mathcal{V}_\Theta = \mathcal{V}_\mathcal{N}^*$  are provided in the next section. The discrepancy we minimise is given by:

$$d_{\mathcal{P}_2^\gamma(\tilde{\mathcal{H}})}(A \odot \nu_u, A \odot \mu_\theta) + d_{\mathcal{P}_2^\gamma(\overline{\mathcal{H}})}(B \odot \nu_u, B \odot \mu_\theta),$$

where  $d_{\mathcal{P}_2^\gamma(\tilde{\mathcal{H}})}$  and  $d_{\mathcal{P}_2^\gamma(\overline{\mathcal{H}})}$  are appropriate metrics defined over the space of probability measures  $\mathcal{P}_2^\gamma(\tilde{\mathcal{H}})$  and  $\mathcal{P}_2^\gamma(\overline{\mathcal{H}})$ , respectively. The variational problem then becomes:

$$\mu_{\theta^*} \in \arg \min_{\mu_\theta \in \mathcal{V}_\mathcal{N}^*} d_{\mathcal{P}_2^\gamma(\tilde{\mathcal{H}})}(A \odot \nu_u, A \odot \mu_\theta) + d_{\mathcal{P}_2^\gamma(\overline{\mathcal{H}})}(B \odot \nu_u, B \odot \mu_\theta). \quad (11)$$

By varying the choice of metrics, neural architectures  $\mathcal{V}_\mathcal{N}$  and the structure of  $X_\theta$ , different approximation strategies can be implemented. Nonetheless, the ultimate objective remains the same: to identify an optimal Neural Measure  $\mu_{\theta^*}$  that is close enough to the target distribution  $\nu_u$ .

## 3 Discrete Neural Measure Spaces

To motivate the definition of neural measures on  $\mathcal{P}(\mathcal{H})$  we consider a family of discrete stochastic mappings

$$\tilde{X}_\theta : \Omega \rightarrow \mathcal{H},$$

where each map  $\tilde{X}_\theta$  is *associated* with a neural network function parameterised by  $\theta \in \Theta$ , where  $\Theta$  indexes a class of neural networks  $\mathcal{V}_\mathcal{N}$ . Our building assumption is that  $\tilde{X}_\theta$  will be based on standard discrete neural spaces  $\mathcal{V}_\mathcal{N}$  designed to approximate functions. The alternative designs we consider are based on neural network functions corresponding to (i) both deterministic  $(x, t)$  and stochastic variables  $(\xi)$ , (ii) only deterministic variables and (iii) only stochastic variables. Thus, each model will be characterised by a function  $g_\theta \in \mathcal{V}_\mathcal{N}$ , and our goal is to approximate the distribution associated to the solution  $u$  by solving an appropriate optimisation problem over  $\Theta$ .

To be more precise, let  $\mathcal{V}_\mathcal{N}$  be a chosen class of neural networks as above, and let  $\gamma$  be the reference probability measure defined on a latent space  $\Xi$ . We define first a corresponding family of functions  $X_\theta = X_\theta(x, t, \xi)$ ,

$$X_\theta : \Xi \rightarrow \mathcal{H},$$

where each model  $X_\theta$  is implicitly determined by a function  $g_\theta \in \mathcal{V}_\mathcal{N}$ , i.e.,  $X_\theta = X(g_\theta)$ . These functions encode the neural architecture and the parameterisation of the model, and will be detailed in the following Sections 3.1-3.

To introduce stochasticity, we consider a random variable  $\xi : \Omega \rightarrow \Xi$ , distributed according to  $\gamma$ . Composing this with the deterministic map  $X_\theta$  yields the stochastic model:

$$\tilde{X}_\theta(\omega) = X_\theta \circ \xi(\omega).$$

This composition defines a random element in  $\mathcal{H}$  allowing us to generate samples from the associated distribution. The pushforward of  $\gamma$  through  $X_\theta$ , denoted by  $[X_\theta]_\# \gamma$ , defines the induced discrete Neural Measure Space on  $\mathcal{P}(\mathcal{H})$ . In fact, the class of Neural Measures spaces we consider have the form,

$$\mathcal{V}_\mathcal{N}^* = \left\{ \mu_\theta = [X_\theta]_\# \gamma \text{ for some Neural Model } X_\theta = X(g_\theta), \quad g_\theta \in \mathcal{V}_\mathcal{N} \right\}.$$

Clearly,  $\mathcal{V}_\mathcal{N}^* \subset \mathcal{P}(\mathcal{H})$  and in fact  $\mathcal{V}_\mathcal{N}^* \subset \mathcal{P}_2^\gamma(\mathcal{H})$ . Here,  $\mathcal{V}_\mathcal{N}$  is fixed a priori, and the notation  $\mathcal{V}_\mathcal{N}^*$  reflects the fact that this space is associated with a discrete standard neural network space  $\mathcal{V}_\mathcal{N}$ . Each model in  $\mathcal{V}_\mathcal{N}^*$  corresponds to a unique pushforward measure derived from a neural map and the reference measure. Notice finally that although  $\xi \sim \gamma$  is sampled from a known reference distribution, its explicit form  $\xi(\omega)$  need not to be specified.

### 3.1 Fully Network Based Neural Measure Spaces

Next, we consider  $X_\theta$ , defined in relation to neural network functions  $g_\theta \in \mathcal{V}_\mathcal{N}$ , corresponding to both deterministic  $(x, t)$  and stochastic variables  $(\xi)$ . The resulting neural models solely rely on a chosen class of neural networks  $\mathcal{V}_\mathcal{N}$  without any further approximation step.

By fixing the number of layers, the size of each hidden layer, and the activation functions, we define the following class

$$\mathcal{V}_\mathcal{N} := \left\{ g_\theta : \mathbb{R}^{d_{in}} \times \mathbb{R}^{d_{ran}} \rightarrow \mathbb{R}^s : g_\theta(x, t; \xi) := C_L \circ \sigma \circ C_{L-1} \cdots \circ \sigma \circ C_1(x, t; \xi) \text{ for } \theta \in \Theta \right\}.$$

In the above procedure, any such map  $g_\theta$  is defined by the intermediate layers  $C_k$ , which are affine maps of the form

$$C_k y = W_k y + b_k, \quad \text{where } W_k \in \mathbb{R}^{d_{k+1} \times d_k}, b_k \in \mathbb{R}^{d_{k+1}}, \quad (12)$$

where the dimensions  $d_k$  may vary with each layer  $k$  and the activation function  $\sigma(y)$  denotes the vector with the same number of components as  $y$ , where  $\sigma(y)_i = \sigma(y_i)$ . The index  $\theta \in \Theta$  represents collectively all the parameters of the network.

Then, we define the neural model as:

$$X_\theta(\xi) = g_\theta(\cdot; \xi), \quad \text{for some } g_\theta \in \mathcal{V}_\mathcal{N}.$$

We may additionally require that for every  $g_\theta \in \mathcal{V}_\mathcal{N}$

- $g_\theta(\cdot, \xi) \in \mathcal{H}$ , for every  $\xi$ ,
- and  $\int_{\Xi} \|g_\theta(\cdot; \xi)\|_{\mathcal{H}}^2 \gamma(d\xi) < \infty$ .

These ensure that  $X_\theta \in L^2(\gamma; \mathcal{H})$ . The associated variational method is optimised based on the following class of Neural Measures:

$$\mathcal{V}_{\mathcal{N}}^* = \left\{ [X_\theta]_{\#} \gamma \in \mathcal{P}_p^\gamma(\mathcal{H}) : \text{ where } X_\theta(\xi) = g_\theta(\cdot, \xi) \text{ for some } g_\theta \in \mathcal{V}_{\mathcal{N}} \right\}.$$

This formulation is simple and general—it captures a wide range of model classes without assuming any structure other than that provided by the neural network architecture itself. The construction presented is typical, and several alternative architectures are feasible; it is presented in this specific form for completeness of exposition.

### 3.2 PCE-NN Based Neural Measure Spaces

In this section, we introduce a class of neural models designed to approximate functions  $U \in L^2(\gamma; \mathcal{H})$ , where the computational complexity of learning high-dimensional mappings  $(x, t; \xi) \mapsto \mathbb{R}^s$  is reduced through truncated spectral expansion. The key idea is to exploit the linear structure of the Hilbert space  $L^2(\gamma; \mathcal{H})$  and separate the stochastic and deterministic components of the function.

To this end, consider a Polynomial Chaos Expansion (PCE)-type basis, [42],  $\{\phi_n\}_{n \in \mathbb{N}} \subset L^2(\gamma)$  satisfying:

$$\forall q \in L^2(\gamma; \mathcal{H}), \quad \exists! \{a_n\}_{n \in \mathbb{N}} \subset \mathcal{H} : \quad q(x, t; \xi) = \sum_{n \in \mathbb{N}} a_n(x, t) \phi_n(\xi), \quad (13)$$

we represent the neural model as a truncated expansion:

$$X_\theta(\xi) = \sum_{n=1}^K g_\theta^{(n)} \phi_n(\xi),$$

where each coefficient function  $g_\theta^{(n)} \in \mathcal{H}$  is a component of the output layer of some neural network  $g_\theta$  within  $\mathcal{V}_{\mathcal{N}}$ , i.e.

$$\mathcal{V}_{\mathcal{N}} := \left\{ g_\theta : \mathbb{R}^{d_{input}} \rightarrow \mathbb{R}^{d_{out}K} : g_\theta = g_\theta(x, t) \text{ for } \theta \in \Theta \right\},$$

and the structure of the neural network functions  $g_\theta(x, t)$  is as before, but now affecting only  $x, t$  variables. Then the corresponding form of neural measures is:

$$\mathcal{V}_{\mathcal{N}}^* = \left\{ [X_\theta]_{\#} \gamma \in \mathcal{P}_2^\gamma(\mathcal{H}) : \text{ where } X_\theta(\xi) = \sum_{n=1}^K g_\theta^{(n)} \phi_n(\xi) \text{ for some } g_\theta \in \mathcal{V}_{\mathcal{N}} \right\}.$$

This construction decouples the stochastic and deterministic components, enabling: simpler and lower-dimensional neural architectures, and possibly structured learning problems.

### 3.3 Galerkin-NN Based Neural Measure Spaces

Galerkin-NNs are conceptually similar to PCE-PINNs but draw inspiration from the Galerkin method used in numerical PDEs. In this approach, the governing equations are projected onto a test basis, and neural networks are formulated accordingly. The architecture closely mirrors that of PCE-NNs, although neural networks are used now for the discretisation of  $\xi$  variable. For this reason, we only present the analogue corresponding to the variant that directly approximates the solution  $U(\xi)$ .



Consider appropriate a given finite dimensional Galerkin subspace of  $\mathcal{H}$ , denoted by  $\mathcal{H}_h$ , let  $M$  be its dimension and  $\{\psi_n\}_1^M$  its basis. Then we consider the elements of  $L^2(\gamma; \mathcal{H})$

$$q(x, t; \xi) = \sum_{n=1}^M b_n(\xi) \psi_n(x, t). \quad (14)$$

Clearly, for each fixed  $\xi$ ,  $q(\cdot; \xi) \in \mathcal{H}_h$ . We then represent the neural model as

$$X_\theta(\xi) = \sum_{n=1}^M g_\theta^{(n)}(\xi) \psi_n,$$

where each coefficient function  $g_\theta^{(n)} \in L^2(\gamma)$  is a component of the output layer of some neural network  $g_\theta$  within  $\mathcal{V}_\mathcal{N}$ , i.e.,

$$\mathcal{V}_\mathcal{N} := \{g_\theta : \mathbb{R}^{d_{ran}} \rightarrow \mathbb{R}^M : g_\theta = g_\theta(\xi) \text{ for } \theta \in \Theta\},$$

and the structure of the neural network functions  $g_\theta(\xi)$  is as before, but now affecting only the  $\xi$  variable. Then the corresponding form of neural measures is:

$$\mathcal{V}_\mathcal{N}^* = \left\{ [X_\theta]_{\#} \gamma \in \mathcal{P}_2^\gamma(\mathcal{H}) : \text{where } X_\theta(\xi) = \sum_{n=1}^M g_\theta^{(n)}(\xi) \psi_n \text{ for some } g_\theta \in \mathcal{V}_\mathcal{N} \right\}.$$

Although the above formulation is quite flexible and compatible with more standard methods for the numerical solution of PDEs, its actual implementation depends on the choice of the spaces  $\mathcal{H}_h$ . It is possible using the Discontinuous Galerkin framework, to consider spaces that are not subspaces of  $\mathcal{H}$ . This approach is more involved and is beyond the scope of this work.

## 4 Distances and their evaluation

In statistical learning and probabilistic modeling, measuring the "distance" between probability measures is a fundamental task. Two broad families of such distances are commonly used: divergences and metrics, both of which serve to quantify dissimilarity over a suitable space of probability measures, such as  $\mathcal{P}(\mathcal{H})$ . Depending on the nature of the problem, several alternative choices can be made, resulting in different loss functions. Our framework is flexible in this regard. We will focus next on Wasserstein distances, as in this case, the loss function takes a particular simple form.

### 4.1 Loss based on Wasserstein distance

Within the framework the present paper it is particularly convenient to consider Wasserstein distances. A key observation is that when one of the measures to be used in the loss is atomic, i.e.,  $\delta_g$ , then the set of plans is reduced to  $\mu \times \delta_g$ , i.e.,  $\Pi(\mu, \delta_g) = \{\mu \times \delta_g\}$ , see (5.2.12) in [2]. Assuming  $g \in \mathcal{H}$  and  $\delta_g \in \mathcal{P}_p(\mathcal{H})$ , we then have

$$\begin{aligned} W_p(\mu, \delta_g)^p &= \inf_{\pi \in \Pi(\mu, \delta_g)} \int_{\mathcal{H}} \int_{\mathcal{H}} \|x - y\|_{\mathcal{H}}^p \pi(\mathrm{d}x, \mathrm{d}y) = \int_{\mathcal{H}} \int_{\mathcal{H}} \|x - y\|_{\mathcal{H}}^p \mu(\mathrm{d}x) \delta_g(\mathrm{d}y) \\ &= \int_{\mathcal{H}} \|x - g\|_{\mathcal{H}}^p \mu(\mathrm{d}x) = \mathbb{E}_{X \sim \mu} \|X - g\|_{\mathcal{H}}^p \end{aligned} \quad (15)$$

We distinguish two cases. In case where  $\mathcal{AU}(\xi)$  and  $\mathcal{BU}(\xi)$  are constant with respect to  $\xi$ , we can easily check exists  $f \in \tilde{\mathcal{H}}$  and  $g \in \overline{\mathcal{H}}$  such that

$$A \odot \nu_u = \delta_f, \quad B \odot \nu_u = \delta_g,$$

and the suggested variational method can be written as follows:

$$\mu_{\theta^*} \in \arg \min_{\mu_{\theta} \in \mathcal{V}_{\mathcal{N}}^*} W_p(A \odot \mu_{\theta}, \delta_f) + W_p(B \odot \mu_{\theta}, \delta_g).$$

In the general case, it is still possible to use this property if we define residual operators

$$\tilde{A}_{\xi} X_{\theta}(\xi) := \mathcal{A}X_{\theta}(\xi) - \mathcal{A}U_{\theta}(\xi), \quad \text{and} \quad \tilde{B}_{\xi} X_{\theta}(\xi) := \mathcal{B}X_{\theta}(\xi) - \mathcal{B}U_{\theta}(\xi),$$

and the suggested variational method can be written as follows:

$$\mu_{\theta^*} \in \arg \min_{\mu_{\theta} \in \mathcal{V}_{\mathcal{N}}^*} W_p(\tilde{A} \odot \mu_{\theta}, \delta_0) + W_p(\tilde{B} \odot \mu_{\theta}, \delta_0).$$

This is particularly helpful, since the computation of the Wasserstein distances in both cases is reduced to ( $p = 2$ ) the evaluation of integrals of functions,

$$d_{2,\gamma}(A \odot \nu_u, A \odot \mu_{\theta})^2 + d_{2,\gamma}(B \odot \nu_u, B \odot \mu_{\theta})^2 = \|\mathcal{A}U - \mathcal{A}X_{\theta}\|_{L^2(\gamma; \tilde{\mathcal{H}})}^2 + \|\mathcal{B}U - \mathcal{B}X_{\theta}\|_{L^2(\gamma; \overline{\mathcal{H}})}^2.$$

In fact, recall that both  $\nu_u, \mu_{\theta} \in \mathcal{P}_2^{\gamma}(\mathcal{H})$ . Additionally, by hypothesis (7), it follows that  $A \odot \nu_u, A \odot \mu_{\theta} \in \mathcal{P}_2^{\gamma}(\tilde{\mathcal{H}})$  and  $B \odot \nu_u, B \odot \mu_{\theta} \in \mathcal{P}_2^{\gamma}(\overline{\mathcal{H}})$ .

## 4.2 Other metrics and divergences

It is possible, however, to utilise alternative divergences or metrics to define the loss functional. We briefly review some potential choices below, see, eg., [6, 7, 28, 36, 37, 39, 41].

### 4.2.1 Divergences and Metrics: Definitions and Relationships

Divergences generalise metrics by dropping symmetry and the triangle inequality, while retaining non-negativity and vanishing only when the inputs are equal. A key family is the f-divergences: given probability measures  $\mu \ll \nu$  and a convex function  $f : \mathbb{R}_+ \rightarrow \mathbb{R} \cup \{+\infty\}$  with  $f(1) = 0$ , the  $f$ -divergence is defined as

$$D_f(\mu || \nu) = \int f\left(\frac{d\mu}{d\nu}\right) d\nu.$$

This includes the Kullback–Leibler (KL) divergence, Jensen–Shannon divergence, and others. In addition to divergences, several frameworks exist for constructing metric distances between probability measures. These include:

#### (A) Integral Probability Metric (IPM):

Given a class of test functions  $\mathcal{F}$ , the IPM between two measures  $\mu, \nu$  is defined as:

$$d_{\mathcal{F}}(\mu, \nu) := \sup_{f \in \mathcal{F}} |\mathbb{E}_{X \sim \mu} f(X) - \mathbb{E}_{Y \sim \nu} f(Y)|. \quad (16)$$

#### (B) Optimal Transport (OT) Metrics:

In OT theory, distances are defined via couplings. Given a cost function  $c(x, y)$ , the Wasserstein distance (or more generally,  $c$ -Wasserstein distance) is

$$W_c(\mu, \nu) = \inf_{\pi \in \Pi(\mu, \nu)} \int c(x, y) d\pi(x, y),$$

where  $\Pi(\mu, \nu)$  is the set of couplings of  $\mu$  and  $\nu$ .

#### (C) TV Distance via Densities:

Given a probability measure  $\lambda \in \mathcal{P}(\mathcal{H})$ , we define  $\mathcal{P}_{\lambda}(\mathcal{H}) \subset \mathcal{P}(\mathcal{H})$  to be the collection of probability measures that are absolutely continuous with respect to  $\lambda$ , ie.  $\mu \ll \lambda$ . Let  $\mu, \nu \in \mathcal{P}_{\lambda}(\mathcal{H})$  with Radon–Nikodym derivatives  $f_{\mu}, f_{\nu}$  with respect to  $\lambda$ . Then TV distance between  $\mu, \nu$  can be expressed as:

$$d_{TV}(\mu, \nu) := \frac{1}{2} \|f_{\mu} - f_{\nu}\|_{L^1(\lambda)}.$$

### 4.2.2 Approximating Distances in Finite-Dimensional Spaces

Given that our spaces,  $V_\Theta = V_{\mathcal{N}}^*$ , have a finite number of parameters, we can employ techniques developed in approximating distances of distributions in finite dimensions to compute the actual loss function. Indicative such methods include, GANs and computational optimal transport algorithms, [13, 29].

For approximating Wasserstein distances, one may use Sinkhorn Algorithm which introduces entropic regularisation for efficient computation and other approaches detailed in [29]. These approaches exploit the geometric and variational structure of optimal transport theory and are particularly relevant in generative modelling and distributional approximation tasks.

Generative Adversarial Networks (GANs) provide a flexible variational framework for approximating probability distributions by minimising statistical distances, notably Integral Probability Metrics (IPMs) and, under certain conditions,  $f$ -divergences.

Given a class of generators  $g_\theta \in \mathcal{V}_{\mathcal{N}}$ , a class of discriminators  $f_\phi \in \bar{\mathcal{V}}_{\mathcal{N}}$ , a reference distribution  $\pi_0$  and target distribution  $\mathbb{P}_r$  the standard GAN objective takes the form:

$$\min_{g_\theta \in \mathcal{V}_{\mathcal{N}}} \max_{f_\phi \in \bar{\mathcal{V}}_{\mathcal{N}}} \mathbb{E}_{X \sim \mathbb{P}_r} f_\phi(X) - \mathbb{E}_{Z \sim \pi_0} f_\phi \circ g_\theta \circ (Z).$$

In the special case where the class of test functions  $\mathcal{F}$  associated with a particular IPM (eg. as in equation (16)) can be approximated by the class of discriminators  $\bar{\mathcal{V}}_{\mathcal{N}}$ . Then, this min-max formulation can be viewed as minimising IPM between  $\mathbb{P}_r$  and generators distribution. Specifically, we define the class of neural measures:

$$\mathcal{V}_{\mathcal{N}}^* := \left\{ [g_\theta]_{\#} \pi_0 : \text{for some } g_\theta \in \mathcal{V}_{\mathcal{N}} \right\}.$$

where  $[g_\theta]_{\#} \pi_0$  is the law of the distribution  $g_\theta \circ (Z)$  when  $Z \sim \pi_0$ . The above min-max formulation provides a way to approximate the variational problem:

$$\arg \min_{\mu_\theta \in \mathcal{V}_{\mathcal{N}}^*} d_{\mathcal{F}}(\mathbb{P}_r, \mu_\theta), \quad \text{where } d_{\mathcal{F}} \text{ is the IPM induced by the class } \mathcal{F}.$$

## 5 Numerical results

In this section, we present numerical experiments that illustrate the performance of the methods introduced in Sections 2 and 3. We consider three representative examples: a bistable ordinary differential equation (ODE), a diffusion partial differential equation (PDE), and a reaction-diffusion PDE. In all cases, the problem parameters are treated as random variables drawn from prescribed distributions, and the objective is to quantify the resulting uncertainty in the solution.

All neural networks employed are fully connected multi-layer perceptrons (MLPs). The architectures used in the three examples consist of 5, 6, and 6 hidden layers, with 32, 20, and 40 hidden units per layer, respectively. We use the sinusoidal-based activation function known as the snake activation, defined as

$$\sigma(x; a) = x + \frac{\sin^2(ax)}{a},$$

following [49]. This choice consistently yielded better convergence and expressiveness than the traditional hyperbolic tangent activation, especially for problems involving both periodic and non-periodic solutions. The parameter  $a$  is specific to each layer and is optimized jointly with the network weights during training.

Training is performed using the L-BFGS optimizer with a learning rate of 1, a maximum number of iterations set to 20, and a history size of 20. No batch processing is used; the optimizer is applied to the full dataset at each step. We initialize the weights using Xavier initialization.

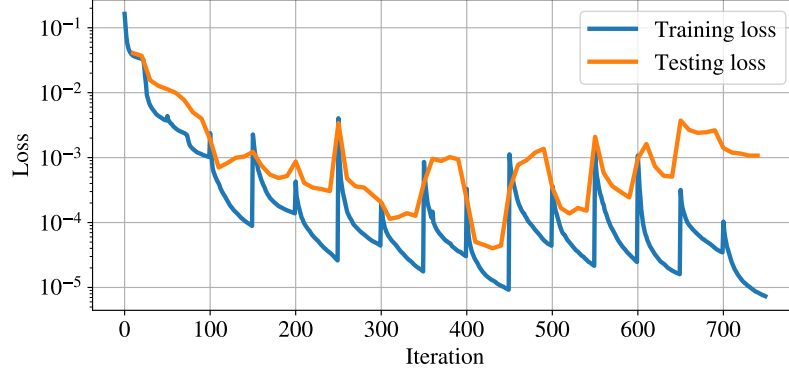


Figure 1: Training and testing loss over time during the training of the PINN architecture for the bistable ODE (17).

Training samples from the spatiotemporal domain of the differential equation are resampled every predefined number of iterations, while samples from the parameter space are resampled every different predefined interval. The resampling frequency for the domain is higher than that for the parameter space. This strategy allows the network to first focus on learning the PDE structure for a specific parameter configuration and later generalize to new configurations as training progresses.

All experiments were conducted using a unified codebase, which is publicly available at [3], ensuring reproducibility and ease of extension to other problem settings.

### 5.1 Bistable ordinary differential equation

We consider the ordinary differential equation,

$$\frac{du}{dt} = -r(u-1)(2-u)(y-3), \quad t \in [0, 8], \quad (17)$$

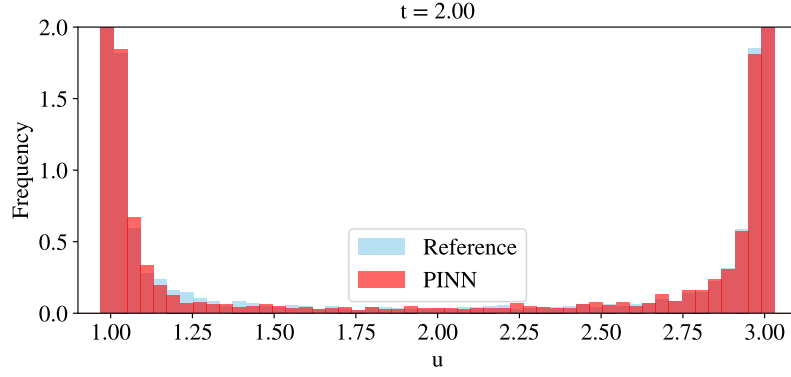
with initial condition,

$$u(0) = u_0. \quad (18)$$

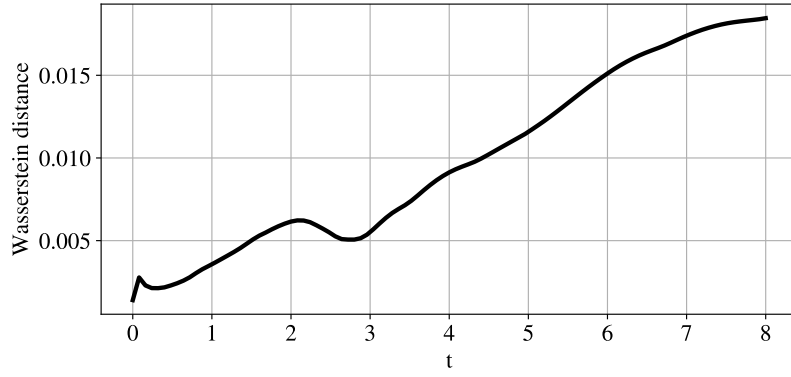
The parameters  $u_0, r$  follow uniform distributions,  $y_0 \sim \mathcal{U}(0, 4)$  and  $r \sim \mathcal{U}(0.8, 1.2)$ . The equation has two stable ( $u = 1, u = 3$ ) and one unstable ( $u = 2$ ) equilibrium solutions.

In Figure 1, we plot the training and testing loss functions throughout the optimization. The spatial-temporal domain is resampled every 50 iterations, as are the parameters, which are drawn from their predefined uniform distribution. Each resampling uses 100 random samples from the domain. After each resampling step, the loss typically spikes due to the shift in training data but continues to decrease overall as training progresses. The testing loss begins to rise after around 400 iterations, indicating that the network starts to overfit the training data.

In Figure 2, we plot histograms of the solution to the bistable ODE (17). The reference solution is obtained using an implicit numerical solver. We observe good qualitative agreement between the reference and the PINN-based histograms. However, the Wasserstein distance between the two solutions increases over time. This is expected, as the solution's distribution gradually concentrates into two Dirac delta peaks at  $u = 1$  and  $u = 3$ . This sharp concentration makes convergence challenging, since the Wasserstein distance is highly sensitive to samples that have not fully collapsed onto the Dirac masses.



(a) Histogram comparison.



(b) Wasserstein distance over time.

Figure 2: Histograms at time  $t = 2$  and Wasserstein distance between the histograms over the time interval  $[0, 8]$  of the solution of the bistable ODE (17) using an implicit numerical solver and the PINN architecture for different parameter values.

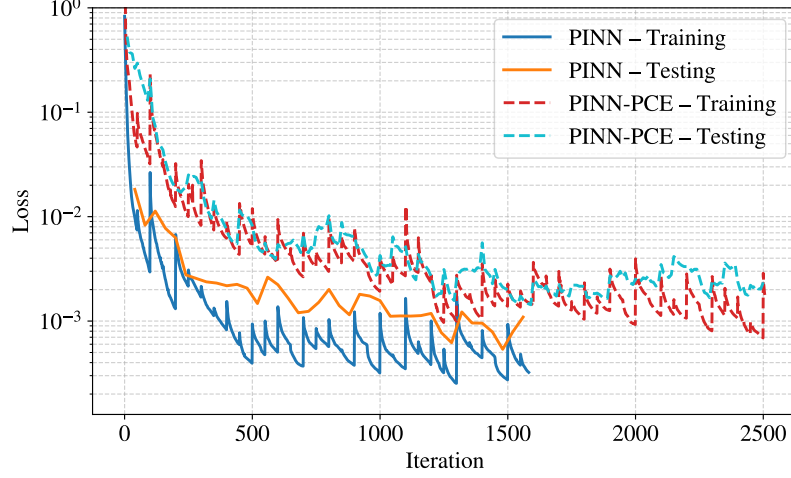


Figure 3: Training and testing loss function over time of the training of the PINN and the PINN-PCE architecture for the diffusion equation (19).

## 5.2 Diffusion equation

We solve the diffusion equation

$$u_t - \frac{a}{k^2} u_{xx} = 0, \quad t \in [0, 1], \quad x \in [0, \pi]. \quad (19)$$

with initial and boundary conditions,

$$u(0, x) = \sin(kx), \quad x \in [0, \pi], \quad (20)$$

$$u(t, 0) = 0, \quad t \in [0, 1], \quad (21)$$

$$u(t, \pi) = e^{-at} \sin(\pi k), \quad t \in [0, 1], \quad (22)$$

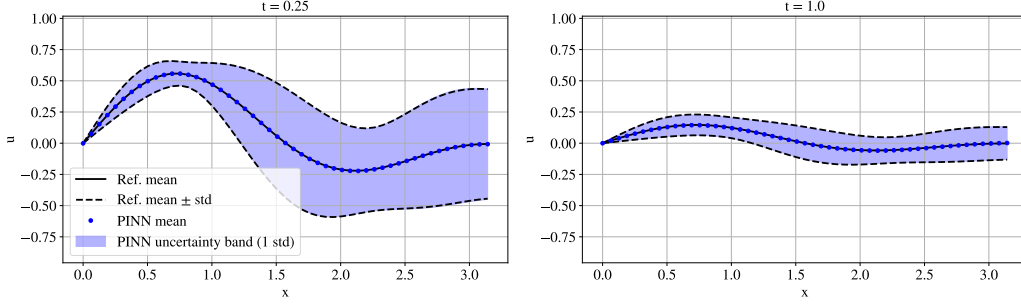
and exact solution,

$$u(t, x) = e^{-kt} \sin(\pi x). \quad (23)$$

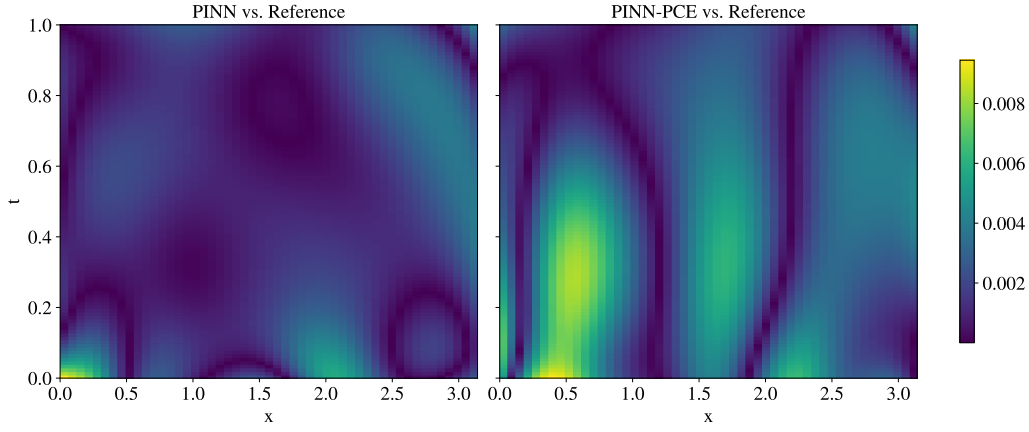
We assume that the parameters  $a, k$  follow uniform distributions,  $a \sim \mathcal{U}(1, 3)$  and  $k \sim \mathcal{U}(1, 3)$ .

In Figure 3, we plot the training and testing loss functions during the training of both the PINN and PINN-PCE architectures for the diffusion equation (19). The spatial-temporal domain is resampled every 50 iterations, while the parameters are resampled every 100 iterations. The domain is sampled by selecting 20 spatial and 10 temporal points, forming a Cartesian product of 200 training locations. The PCE basis used in the PINN-PCE model consists of orthogonal polynomials up to degree 5. We observe that the training and testing errors of the PINN-PCE model are consistently higher than those of the plain PINN model. This behavior remains even when increasing the degree of the PCE basis.

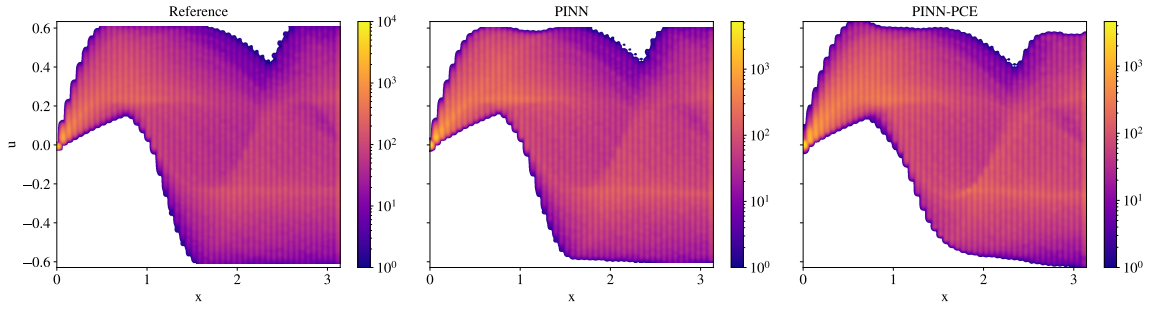
In Figure 4, we present the average solution and histograms for the diffusion equation (19) at time  $t = 0.5$ , computed using the PINN and PINN-PCE architectures. In Figure 4a, the x-axis represents the spatial coordinate and the y-axis corresponds to time. Figure 4b displays the spatial coordinate on the x-axis and the logarithm of the frequency of solution values on the y-axis. We observe that the PINN-PCE architecture yields slightly improved results compared to the plain PINN. Both methods show good qualitative agreement with the analytical solution, indicating their capacity to learn the underlying dynamics of the equation.



(a) Mean and standard deviation of the reference and PINN-based solutions.



(b) Average values comparison.



(c) Histogram comparison at time  $t = 0.5$ .

Figure 4: Average and one standard deviation of the reference and PINN-based solutions (a), at time  $t = 0.5$  and  $t = 1$ . Average values (b) and histograms of the solution (c) of the diffusion equation (19) at time  $t = 0.5$  using the PINN and the PINN-PCE architectures. Notice that PINN produces marginally better results than the PINN-PCE architecture.

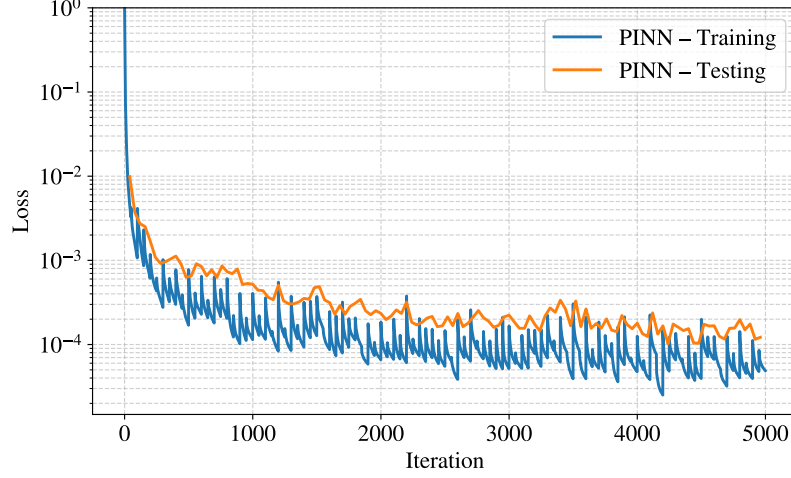


Figure 5: Training and testing loss function over time of the training of the PINN and the PINN-PCE architecture for the reaction-diffusion equation (25).

### 5.3 Reaction-Diffusion

We consider the partial differential equation,

$$u_t - Du_{xx} + gu^3 = f, \quad t \in [0, 4], \quad x \in [-1, 1], \quad (24)$$

with initial and boundary conditions,

$$u(0, x) = 0.5 \cos^2(\pi x), \quad (25)$$

$$u(t, -1) = u(t, 1) = 0.5. \quad (26)$$

The reaction function  $g$  is given by,

$$g(x) = 0.2 + e^{r_1 x} \cos^2(r_2 x), \quad (27)$$

with  $r_1 \sim \mathcal{U}(0.5, 1)$  and  $r_2 \sim \mathcal{U}(3, 4)$  and the forcing function is given by,

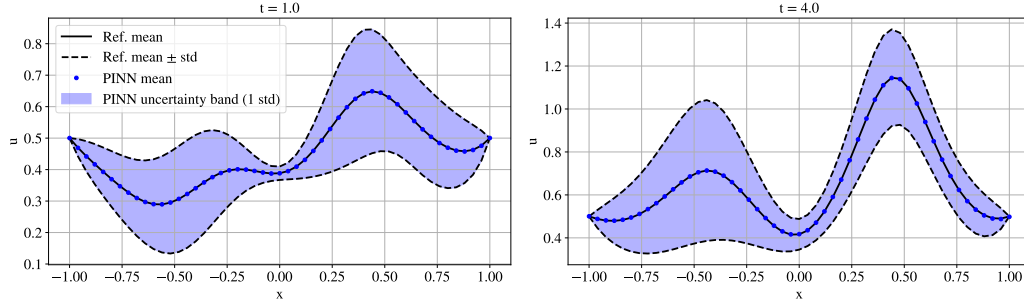
$$f(x) = \exp\left(-\frac{(x - 0.25)^2}{2k_1^2}\right) \sin^2(k_2 x), \quad (28)$$

with  $k_1 \sim \mathcal{U}(0.2, 0.8)$  and  $k_2 \sim \mathcal{U}(1, 4)$ . The diffusion coefficient is fixed to  $D = 0.01$ . This equation has been studied in [31].

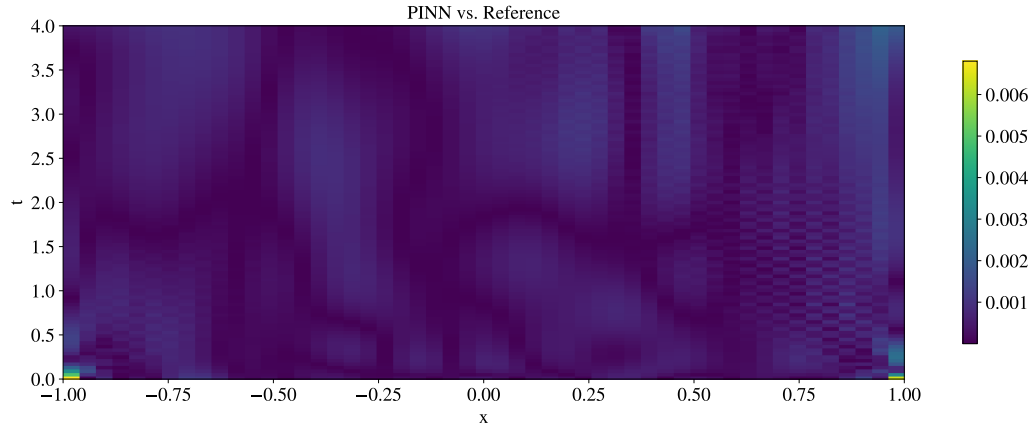
In Figure 5, we plot the training and testing loss functions during the training of the PINN architecture for the reaction-diffusion equation (25). The spatial-temporal domain is resampled every 50 iterations, while the parameters are resampled every 100 iterations. The domain is sampled by selecting 40 spatial and 20 temporal points, forming a Cartesian product of 800 training locations.

In Figure 6, we plot the mean and standard deviation of the reference and PINN-based solutions. The absolute error heatmap shows that the PINN-based solution is in good qualitative agreement with the reference solution. The histograms of the solution at  $t = 2$  show that the PINN-based solution is in good qualitative agreement with the reference solution. The error shown in Figure 6b shows larger values at the boundaries of the domain for initial times. This flaw can probably be fixed by using adaptive selection of the training points based on the error.

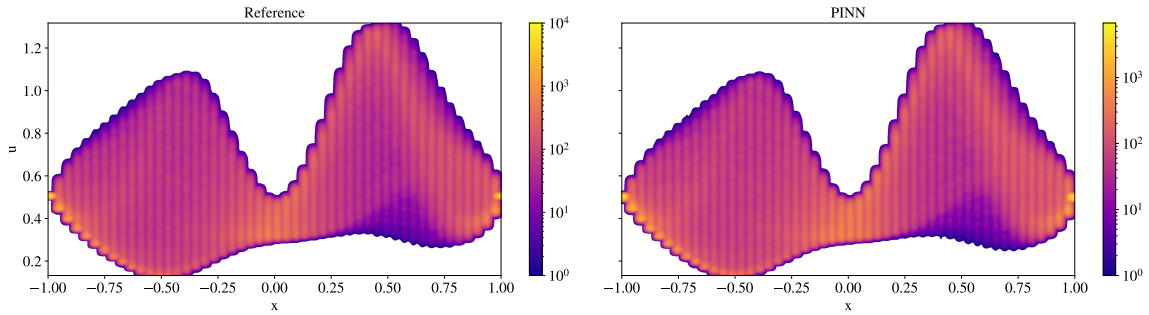




(a) Mean and standard deviation of the reference and PINN-based solutions.



(b) Absolute error heatmap.



(c) Histograms of the solution at time  $t = 2$ .

Figure 6: Average values and histograms of the solution of the reaction-diffusion equation (25) at time  $t = 2$  using the PINN architecture. The statistics produced by the PINN architecture are in good qualitative agreement with the reference solution.

## 6 Technical Remarks

### 6.1 Well-Definedness of $U(\xi)$ Distribution

Based on the Random PDE stated in (6), we are interested in approximating its probability distribution, namely  $[U]_{\#} \gamma$ . We would like to know under what assumptions can we ensure that this distribution is well-defined. Moreover, does  $[U]_{\#} \gamma$  depend on the choice of the underlying probability space  $(\Omega, \mathcal{F}, \mathbb{P})$ ?

To answer this, we first define two mappings. Given a stochastic process

$$f : D \times \Xi \rightarrow \mathbb{R} \quad \text{with} \quad f(\cdot; \xi) \in \tilde{\mathcal{H}},$$

and

$$g : \Gamma \times \Xi \rightarrow \mathbb{R} \quad \text{with} \quad g(\cdot; \xi) \in \overline{\mathcal{H}},$$

we define the evaluation map

$$Q_{f,g} : \Xi \rightarrow \tilde{\mathcal{H}} \times \overline{\mathcal{H}} \times \Xi \quad \text{with} \quad \xi \mapsto (f(\cdot; \xi), g(\cdot; \xi), \xi).$$

Next, we introduce the solution operator

$$G : \tilde{\mathcal{H}} \times \overline{\mathcal{H}} \times \Xi \rightarrow \mathcal{H} \quad \text{with} \quad (\tilde{f}, \tilde{g}, \tilde{\xi}) \mapsto \tilde{u}(\cdot; \tilde{\xi}),$$

where  $\tilde{u}(\cdot; \xi)$  is the solution to the Random PDE (similar to the one in (6)) for a fixed  $\xi = \tilde{\xi}$ , and with right hand side replaced by  $\tilde{f}$  and  $\tilde{g}$ .

Then, the solution  $U(\xi)$  to the original problem can be represented as:

$$U(\xi) = G(f(\cdot; \xi), g(\cdot; \xi), \xi) = G \circ Q_{f,g}(\xi).$$

A sufficient condition for ensuring both the well-definedness of  $[U]_{\#} \gamma$  and its invariance with respect to the abstract probability space  $(\Omega, \mathcal{F}, \mathbb{P})$  is the following:

- The solution operator  $G$  is well-defined for every point in  $\tilde{\mathcal{H}} \times \overline{\mathcal{H}} \times \Xi$ , and
- The composition  $G \circ Q_{f,g}(\xi)$  is measurable on each instance of  $(f, g) \in L^2(\gamma; \tilde{\mathcal{H}}) \times L^2(\gamma; \overline{\mathcal{H}})$ .

Under these conditions, it follows that for any two probability spaces  $(\Omega, \mathcal{F}, \mathbb{P})$  and  $(\tilde{\Omega}, \tilde{\mathcal{F}}, \tilde{\mathbb{P}})$ , with corresponding random elements  $\xi : \Omega \rightarrow \Xi$  and  $\tilde{\xi} : \tilde{\Omega} \rightarrow \Xi$ , both having law  $\gamma$ , we have:

$$[U \circ \xi]_{\#} \mathbb{P} = [G \circ Q_{f,g} \circ \xi]_{\#} \mathbb{P} = [G \circ Q_{f,g}]_{\#} \gamma = [G \circ Q_{f,g} \circ \tilde{\xi}]_{\#} \tilde{\mathbb{P}} = [U \circ \tilde{\xi}]_{\#} \tilde{\mathbb{P}}.$$

This confirms that the push-forward measure  $[U]_{\#} \gamma$  is independent of the choice of the underlying probability space, provided the stated conditions are met.

### 6.2 Discrete Neural Network Spaces

We describe our notation regarding the generic discrete neural network spaces which we denote by  $V_{\mathcal{N}}$ . These are spaces approximating functions

$$v : \mathbb{R}^{d_I} \rightarrow \mathbb{R}^{d_O}.$$

We have used different choices for  $d_I$  and  $d_O$  throughout this paper. To fix ideas, we present a generic structure of the spaces  $V_{\mathcal{N}}$ . Of course several alternative architectures are possible. A *deep neural network* maps every point  $\bar{y} \in \mathbb{R}^{d_I}$  to  $v_{\theta}(\bar{y}) \in \mathbb{R}^{d_O}$ , through

$$v_{\theta}(\bar{y}) = \mathcal{C}_L(\bar{y}) := C_L \circ \sigma \circ C_{L-1} \cdots \circ \sigma \circ C_1(\bar{y}) \quad \forall \bar{y} \in \mathbb{R}^{d_I}. \quad (29)$$

The intermediate layers  $C_k$ , are affine maps of the form

$$C_k y = W_k y + b_k, \quad \text{where } W_k \in \mathbb{R}^{d_{k+1} \times d_k}, b_k \in \mathbb{R}^{d_{k+1}}, \quad (30)$$

where the dimensions  $d_k$  may vary with each layer  $k$  and  $\sigma(y)$  denotes the vector with the same number of components as  $y$ , where  $\sigma(y)_i = \sigma(y_i)$ . The index  $\theta$  represents collectively all the parameters of the network. The space of parameters is denoted by  $\Theta$ :

$$\Theta = \{\theta := (b_1, W_1, \dots, W_L, b_L) : \text{for } b_i \in \mathbb{R}^{d_k}, W_i \in \mathbb{R}^{d_{k+1} \times d_k}, k = 1, \dots, L\}.$$

The set of networks  $\mathcal{C}_L$  with a given architecture of the form (29), (12) is called  $\mathcal{N}$ . Then  $\Theta \in \mathbb{R}^{\dim \mathcal{N}}$  where the total number of degrees of freedom of  $\mathcal{N}$ , is  $\dim \mathcal{N} = \sum_{k=1}^L d_{k+1}(d_k + 1)$ . The nonlinear discrete set of functions  $V_{\mathcal{N}}$  is defined as

$$V_{\mathcal{N}} = \{u_{\theta} : \Omega_T \rightarrow \mathbb{R}, \text{ where } u_{\theta}(x) = \mathcal{C}_L(x), \text{ for some } \mathcal{C}_L \in \mathcal{N}\}. \quad (31)$$

### 6.3 Neural Networks with Random Input as Generative Models

In generative modeling, neural networks receive both a standard input and a random input (often called the latent code or noise). Formally, assume a probability distribution  $\gamma$  over  $\mathbb{R}^{d_{\text{random}}}$  (also known as the seed or reference distribution), and a neural network  $g_{\theta} \in \mathcal{V}_{\mathcal{N}}$ . Then, the generative model is the random variable:

$$g_{\theta}(x; \xi), \quad \text{where } \xi \sim \gamma.$$

This induces a probability distribution over outputs, defined via the pushforward measure:

$$g_{\theta}(x; \xi) \sim [g_{\theta}(x, \cdot)]_{\#} \gamma.$$

To simplify notation, define:

$$Q_{\theta, x}(\xi) := g_{\theta}(x, \xi)$$

Then, the output distribution for a fixed input  $x$  is:

$$\mu_{\theta}(x, A) := \gamma \circ Q_{\theta, x}^{-1}(A) = \int_{\mathbb{R}^{d_{\text{random}}}} \mathbb{1}_{\{g_{\theta}(x, \xi) \in A\}} \gamma(d\xi), \quad \forall A \in \mathcal{B}(\mathbb{R}^{d_{\text{output}}}).$$

If the mapping  $g_{\theta} : \mathbb{R}^{d_{\text{input}}} \times \mathbb{R}^{d_{\text{random}}} \rightarrow \mathbb{R}^{d_{\text{output}}}$  is measurable with respect to the Borel  $\sigma$ -algebras  $\mathcal{B}(\mathbb{R}^{d_{\text{input}}} \times \mathbb{R}^{d_{\text{random}}})$  and  $\mathcal{B}(\mathbb{R}^{d_{\text{output}}})$ , then the following properties hold:

- For every fixed  $x \in \mathbb{R}^{d_{\text{input}}}$ ,  $\mu_{\theta}(x, \cdot)$  is a probability measure on  $\mathbb{R}^{d_{\text{output}}}$
- For every fixed  $A \in \mathcal{B}(\mathbb{R}^{d_{\text{output}}})$ , the function  $x \mapsto \mu_{\theta}(x, A)$  is measurable with respect to  $\mathcal{B}(\mathbb{R}^{d_{\text{input}}})$ .
- $\mu_{\theta}(\cdot, A)$  is  $\mathcal{B}(\mathbb{R}^{d_{\text{input}}}) / \mathcal{B}(\mathbb{R}^{d_{\text{output}}})$ -measurable

Therefore,  $g_{\theta}$  defines a stochastic kernel  $\mu_{\theta}(x, dy)$  from  $\mathbb{R}^{d_{\text{input}}}$  to  $\mathbb{R}^{d_{\text{output}}}$ .

To establish these properties, one can utilise the fact that

$$\mathcal{B}(\mathbb{R}^{d_{\text{input}}} \times \mathbb{R}^{d_{\text{random}}}) = \mathcal{B}(\mathbb{R}^{d_{\text{input}}}) \otimes \mathcal{B}(\mathbb{R}^{d_{\text{random}}}),$$

since both  $\mathbb{R}^{d_{\text{input}}}$  and  $\mathbb{R}^{d_{\text{random}}}$  are Polish spaces, see Theorem 17.25 in [16].

## References

- [1] J. Adler and S. Lunz. “Banach wasserstein gan”. *Advances in neural information processing systems* 31 (2018).
- [2] L. Ambrosio, N. Gigli, and G. Savaré. *Gradient flows in metric spaces and in the space of probability measures*. Lectures in Mathematics ETH Zürich. Birkhäuser Verlag, Basel, 2005, pp. viii+333.
- [3] G. Arampatzis. *measure-uq: Uncertainty Quantification for Physics-Informed Models*. <https://github.com/arampatzis/measure-uq>. Accessed: 2025-06-13. 2024.
- [4] M. Arjovsky, S. Chintala, and L. Bottou. *Wasserstein GAN*. 2017. arXiv: 1701.07875 [stat.ML].
- [5] J. Berg and K. Nyström. “A unified deep artificial neural network approach to partial differential equations in complex geometries”. *Neurocomputing* 317 (Nov. 2018), pp. 28–41.
- [6] J. Birrell, P. Dupuis, M. A. Katsoulakis, Y. Pantazis, and L. Rey-Bellet. “(f, Gamma)-Divergences: Interpolating between f-Divergences and Integral Probability Metrics”. *Journal of machine learning research* 23.39 (2022), pp. 1–70.
- [7] J. Birrell, M. A. Katsoulakis, and Y. Pantazis. “Optimizing Variational Representations of Divergences and Accelerating Their Statistical Estimation”. *IEEE Transactions on Information Theory* 68.7 (2022), pp. 4553–4572.
- [8] A. Creswell, T. White, V. Dumoulin, K. Arulkumaran, B. Sengupta, and A. A. Bharath. “Generative adversarial networks: An overview”. *IEEE signal processing magazine* 35.1 (2018), pp. 53–65.
- [9] M. Dashti and A. M. Stuart. “The Bayesian Approach to Inverse Problems”. *Handbook of Uncertainty Quantification*. Ed. by R. Ghanem, D. Higdon, and H. Owhadi. Cham: Springer International Publishing, 2017, pp. 311–428.
- [10] J. V. Figueres, J. Vanderhaeghen, F. Bragone, K. Morozovska, and K. Shukla. *PINN - a Domain Decomposition Method for Bayesian Physics-Informed Neural Networks*. 2025. arXiv: 2504.19013 [cs.LG].
- [11] Y. Gal, P. Koumoutsakos, F. Lanusse, G. Louppe, and C. Papadimitriou. “Bayesian uncertainty quantification for machine-learned models in physics”. *Nature Reviews Physics* 4.9 (2022), pp. 573–577.
- [12] R. Gao, Y. Wang, M. Yang, and C. Chen. “PI-VEGAN: Physics Informed Variational Embedding Generative Adversarial Networks for Stochastic Differential Equations”. *arXiv preprint arXiv:2307.11289* (2023).

- [13] I. J. Goodfellow, J. Pouget-Abadie, M. Mirza, B. Xu, D. Warde-Farley, S. Ozair, A. Courville, and Y. Bengio. “Generative adversarial nets”. *Advances in neural information processing systems* 27 (2014).
- [14] M. V. de Hoop, D. Z. Huang, E. Qian, and A. M. Stuart. “The cost-accuracy trade-off in operator learning with neural networks”. *arXiv preprint arXiv:2203.13181* (2022).
- [15] L. V. Jospin, H. Laga, F. Boussaid, W. Buntine, and M. Bennamoun. “Hands-on Bayesian neural networks—A tutorial for deep learning users”. *IEEE Computational Intelligence Magazine* 17.2 (2022), pp. 29–48.
- [16] A. Kechris. *Classical descriptive set theory*. Vol. 156. Springer Science & Business Media, 2012.
- [17] D. P. Kingma and M. Welling. “An Introduction to Variational Autoencoders”. *Foundations and Trends in Machine Learning* 12.4 (2019), pp. 307–392.
- [18] N. Kovachki, Z. Li, B. Liu, K. Azizzadenesheli, K. Bhattacharya, A. Stuart, and A. Anandkumar. “Neural operator: Learning maps between function spaces with applications to pdes”. *Journal of Machine Learning Research* 24.89 (2023), pp. 1–97.
- [19] N. B. Kovachki, S. Lanthaler, and A. M. Stuart. “Operator learning: Algorithms and analysis”. *arXiv preprint arXiv:2402.15715* (2024).
- [20] I. Lagaris, A. Likas, and D. Fotiadis. “Artificial neural networks for solving ordinary and partial differential equations”. *IEEE Transactions on Neural Networks* 9.5 (1998), pp. 987–1000.
- [21] Z. Li, N. Kovachki, K. Azizzadenesheli, B. Liu, K. Bhattacharya, A. Stuart, and A. Anandkumar. “Fourier neural operator for parametric partial differential equations”. *arXiv preprint arXiv:2010.08895* (2020).
- [22] X. Liu, W. Yao, W. Peng, and W. Zhou. “Bayesian physics-informed extreme learning machine for forward and inverse PDE problems with noisy data”. *Neurocomputing* 549 (Sept. 2023), p. 126425.
- [23] L. Lu, P. Jin, and G. E. Karniadakis. “Deeponet: Learning nonlinear operators for identifying differential equations based on the universal approximation theorem of operators”. *arXiv preprint arXiv:1910.03193* (2019).
- [24] L. Lu, P. Jin, G. Pang, Z. Zhang, and G. E. Karniadakis. “Learning nonlinear operators via DeepONet based on the universal approximation theorem of operators”. *Nature machine intelligence* 3.3 (2021), pp. 218–229.

- [25] E. Magnani, N. Krämer, R. Eschenhagen, L. Rosasco, and P. Hennig. “Approximate Bayesian neural operators: Uncertainty quantification for parametric PDEs”. *arXiv preprint arXiv:2208.01565* (2022).
- [26] C. G. Makridakis, A. Pim, and T. Pryer. *Deep Uzawa for PDE constrained optimisation*. arXiv2410.17359. 2024. arXiv: 2410.17359 [math.NA].
- [27] X. Meng, L. Yang, Z. Mao, J. del Águila Ferrandis, and G. E. Karniadakis. “Learning functional priors and posteriors from data and physics”. *J. Comput. Phys.* 457 (2022), p. 111073.
- [28] A. Müller. “Integral probability metrics and their generating classes of functions”. *Advances in applied probability* 29.2 (1997), pp. 429–443.
- [29] G. Peyré and M. Cuturi. “Computational Optimal Transport: With Applications to Data Science”. *Foundations and Trends® in Machine Learning* 11.5-6 (2019), pp. 355–607.
- [30] Y. Ping, Y. Zhang, and L. Jiang. “Uncertainty Quantification in PEEC Method: A Physics-Informed Neural Networks-Based Polynomial Chaos Expansion”. *IEEE Transactions on Electromagnetic Compatibility* (2024).
- [31] A. F. Psaros, X. Meng, Z. Zou, L. Guo, and G. E. Karniadakis. “Uncertainty Quantification in Scientific Machine Learning: Methods, Metrics, and Comparisons”. *J. Comput. Phys.* 477 (Mar. 2023), p. 111902.
- [32] A. F. Psaros, X. Meng, Z. Zou, L. Guo, and G. E. Karniadakis. “Uncertainty quantification in scientific machine learning: Methods, metrics, and comparisons”. *J. Comput. Phys.* 477 (2023), p. 111902.
- [33] M. Raissi, P. Perdikaris, and G. E. Karniadakis. “Physics-informed neural networks: a deep learning framework for solving forward and inverse problems involving nonlinear partial differential equations”. *J. Comput. Phys.* 378 (2019), pp. 686–707.
- [34] M. Raissi and G. E. Karniadakis. “Hidden physics models: Machine learning of nonlinear partial differential equations”. *J. Comput. Phys.* 357 (Mar. 2018), pp. 125–141.
- [35] B. Raonic, R. Molinaro, T. De Ryck, T. Rohner, F. Bartolucci, R. Alaifari, S. Mishra, and E. de Bézenac. “Convolutional Neural Operators for robust and accurate learning of PDEs”. *Advances in Neural Information Processing Systems*. Ed. by A. Oh, T. Naumann, A. Globerson, K. Saenko, M. Hardt, and S. Levine. Vol. 36. Curran Associates, Inc., 2023, pp. 77187–77200.
- [36] A. Rényi. “On measures of entropy and information”. *Proceedings of the fourth Berkeley symposium on mathematical statistics and probability, volume 1: contributions to the theory of statistics*. Vol. 4. University of California Press. 1961, pp. 547–562.

- [37] P. K. Sen. *Introduction to nonparametric estimation by Alexandre B. Tsybakov*. 2011.
- [38] J. Sirignano and K. Spiliopoulos. “DGM: a deep learning algorithm for solving partial differential equations”. *J. Comput. Phys.* 375 (2018), pp. 1339–1364.
- [39] B. K. Sriperumbudur, K. Fukumizu, A. Gretton, B. Schölkopf, and G. R. Lanckriet. “On integral probability metrics,  $\phi$ -divergences and binary classification”. *arXiv preprint arXiv:0901.2698* (2009).
- [40] A. Unlu and L. Aitchison. “Variational Laplace for Bayesian neural networks”. *arXiv preprint arXiv:2011.10443* (2020).
- [41] C. Villani. *Optimal transport, old and new*. Vol. 338. Grundlehren der mathematischen Wissenschaften [Fundamental Principles of Mathematical Sciences]. Springer-Verlag, Berlin, 2009, pp. xxii+973.
- [42] D. Xiu and G. E. Karniadakis. “The Wiener–Askey Polynomial Chaos for Stochastic Differential Equations”. *SIAM Journal on Scientific Computing* 24.2 (2002), pp. 619–644. eprint: <https://doi.org/10.1137/S1064827501387826>.
- [43] L. Yang, X. Meng, and G. E. Karniadakis. “B-PINNs: Bayesian physics-informed neural networks for forward and inverse PDE problems with noisy data”. *J. Comput. Phys.* 425 (Jan. 2021), p. 109913.
- [44] L. Yang, D. Zhang, and G. E. Karniadakis. “Physics-informed generative adversarial networks for stochastic differential equations”. *SIAM Journal on Scientific Computing* 42.1 (2020), A292–A317.
- [45] B. J. Zhang and M. A. Katsoulakis. *A mean-field games laboratory for generative modeling*. 2023. arXiv: 2304.13534 [stat.ML].
- [46] D. Zhang, L. Guo, and G. E. Karniadakis. *Learning in Modal Space: Solving Time-Dependent Stochastic PDEs Using Physics-Informed Neural Networks*. 2019. arXiv: 1905.01205 [cs.LG].
- [47] D. Zhang, L. Lu, L. Guo, and G. E. Karniadakis. “Quantifying total uncertainty in physics-informed neural networks for solving forward and inverse stochastic problems”. *J. Comput. Phys.* 397 (2019), p. 108850.
- [48] L. Zhang, Y. Zhang, and Y. Gao. *A Wasserstein GAN model with the total variational regularization*. 2018. arXiv: 1812.00810 [cs.CV].
- [49] L. Ziyin, T. Hartwig, and M. Ueda. “Neural Networks Fail to Learn Periodic Functions and How to Fix It”. *Advances in Neural Information Processing Systems* (2020).